

# Energy Efficient Transmission Based on Grouped Spatial Modulation for upstream DSL Systems

Jiankang Zhang, *Senior Member, IEEE*, Chao Xu, *Member, IEEE*, Tong Bai, *Member, IEEE*, Fasong Wang, Shida Zhong,

**Abstract**—The digital Subscriber Line (DSL) remains an important component of heterogeneous networking, especially in historic city-centers, where using optical fibre is less realistic. Recently, the power consumption has become an important performance metric in telecommunication due to the associated environmental issues. In the recent bonding model, customer sites have been equipped with two/four copper pairs, which may be exploited for designing grouped spatial modulation (SM) aiming for reducing the power consumption and mitigating the stubborn crosstalk in DSL communications. Explicitly, we view the two pair copper pairs equipped for each user as a group and propose an energy efficient transmission scheme based on grouped SM strategy for the upstream DSL systems, which is capable of reducing the power consumption of the upstream transmitters by activating a single copper line of each user. More especially, in order to compensate for the potential bit-rate reduction imposed by reducing the number of activated lines, the proposed scheme implicitly delivers “virtual bits” via activating/deactivating the lines in addition to the classic modulation scheme. This is particularly beneficial in the DSL context, because the crosstalk imposed by activating several lines may swamp the desired signal. Furthermore, a pair of near-optimal soft turbo detection schemes are proposed for exploiting the unique properties of the DSL channel in order to eliminate the error propagation problem of SM detection routinely encountered in wireless channels. Both the attainable energy-efficiency and the achievable Bit Error Ratio (BER) are investigated. Our simulation results demonstrate that the proposed group-based SM is capable of outperforming the vectoring scheme both in terms of its energy efficiency for all the examined loop lengths and transmit powers. Moreover, the proposed group-based SM is capable of outperforming the vectoring scheme both in terms of its BER performance in lower frequencies and longer serviced DSL loop lengths.

**Index Terms**—Digital subscriber line, energy-efficiency, spatial modulation, continuous-input continuous-output memoryless channel, discrete-input continuous-output memoryless channel

## I. INTRODUCTION

Digital Subscriber Lines (DSLs) remain the most widespread fixed broadband data transmission medium around the world with more than 300 million users [1], [2] due to its benefits for both the operators and for the subscribers [3], [4]. Where high-cost fibre installations are unaffordable, the widespread fixed copper cable infrastructure is capable of providing a reliable solution for numerous broadband access applications. Traditionally, DSL technology aims for increasing the achievable data rate [5]–[7], whilst minimizing the outage probability of the subscribers [8], [9]. However, due to the power-thirsty nature of immersive multimedia applications, the power consumption has recently become of prime importance in telecommunications. In our specific context, the cable-distribution unit has a limited heat dissipation capability as well as powering capability [10].

Furthermore, there is an increased interest in environmental issues [8]. Hence, the energy efficiency is at the top of the agenda of the various standardization bodies [11], and it is becoming one of the principal design criteria for future networks and their equipment [12], [13].

In this spirit, low-power modes were introduced into the Asymmetric Digital Subscriber Line (ADSL) standard, but unfortunately they exhibited instability in the operator’s network [11]. Further attempts were made by dynamically managing the spectrum for energy minimization in DSL [14]. Instead of solely maximizing the bit rate by Dynamic Spectrum Management (DSM), Wolkerstorfer, *et al.* [11] formulated a global optimization problem for minimizing the Aggregate Transmit Power (ATP) and struck a trade-off between the energy-efficiency and the bit-rate. A unified rate maximization and ATP minimization framework was also designed by Guenach *et al.* [15] in order to strike a compelling trade-off between the bit rate and power consumption. Furthermore, the total power consumption of Line Drivers (LDs) was incorporated into the objective function by Guenach *et al.* in [16], [17], since the line drivers account for 46% of the total power consumption of ADSL 2 and 36% of that in the Very high speed Digital Subscriber Line (VDSL)2.

The power-conscious design of transceivers may also be capable of improving energy efficiency for example by mitigating the interference. In this spirit, Marrocco *et al.* [18] investigated the vectoring scheme’s [19] capability of reducing power consumption and the impact of channel estimation errors imposed on the power consumption was also analyzed. The classical vectoring scheme has to activate all available twisted pairs for achieving multiplexing gain, which is not energy efficient. Maes *et al.* [20] proposed to combine the discontinuous operation with the vectoring scheme in order to reduce the power potentially. By contrast, Spatial Modulation (SM) [21], [22] has been shown to be an energy efficient wireless transmission scheme by activating a single antenna, which is capable of significantly reducing the total power consumption [23] by implicitly exploiting the spatial resources offered by the antenna indices.

Similarly to wireless systems, fixed broadband networks also exploit the classic Multiple-Input Multiple-Output (MIMO) paradigm, since multiple pairs of wires are bundled together in the bonding transmission [24]. Particularly, in several countries, customers sites have been provided with two copper pairs in many place in Europe, where one copper line is for dedicated voice service and the other copper line is for fax or legacy dial-up data access. However, coupling may rise in these bonding transmission due to expanding

bandwidth. The coupling effect is also known as crosstalk in DSL terminology, which significantly limits the achievable data rate [25], [26] and thus it will also impair the energy efficiency of transmission. Reducing the number of activated lines will intuitively mitigate the crosstalk, but it also reduces the aggregate information rate of the cable due to using a limited subset of the available pairs. Hence, our objective in this paper is to reduce the power consumption and mitigate the cross-talk without totally wasting the inactivated lines. This might seem unrealistic at first sight, but we will demonstrate that this ambitious may be achieved by grouping the wirelines for group-based SM transmission.

To expound a little further, in order to maintain a sufficiently high capacity whilst reducing the power consumption, we design an energy efficient scheme with the aid of our grouped SM design philosophy. Explicitly, the proposed grouped SM views the two pair twisted wires equipped for each user as a group, and each group only activates a single pair of wires, whilst exploiting the beneficial feature of SM, namely that extra implicit information is delivered by the indices of the activated wires. More specifically, the novel contributions of this paper are as follows:

- 1) We conceive group-based SM by activating a single twisted pair from two pairs twisted wires of a group, which eliminates the crosstalk imposed by the adjacent pair. However, the *virtual bits* are delivered via the specific twisted pair indices activated in the different groups.
- 2) Furthermore, a pair of soft turbo-detection schemes are proposed. Explicitly, the Column-Wise Diagonal Dominance (CWDD) property [19] of the DSL channel below 102.4 MHz facilitates the low-complexity single-channel-based SM detection for achieving near-optimum performance without encountering the classic error propagation problem of SM detection routinely encountered in wireless channels.
- 3) Furthermore, both the Continuous-input Continuous-output Memoryless Channel (CCMC) and the Discrete-input Continuous-output Memoryless Channel (DCMC) capacity are quantified and the energy efficiency is investigated. The Bit Error Ratio (BER) performance is investigated at a number of representative cut-off frequencies, which span from 26.975 MHz to 101.975 MHz. The total achievable throughput and the overall BER performance attained upon increasing the bandwidth are also investigated for characterizing the overall performance.

Throughout this paper,  $\mathbb{C}$  denotes the complex number field, bold fonts are used to denote matrices and vectors. The transpose and Hermitian transpose operators are denoted by  $(\cdot)^T$  and  $(\cdot)^H$ , respectively. The inverse operation is denoted by  $(\cdot)^{-1}$ , while  $\mathbb{E}\{\cdot\}$  stands for the expectation operations.

The rest of this paper is organized as follows. Section II describes the system model of colorblackthe multi-user upstream DSL systems. Section III presents the proposed group-based SM transmission scheme as well as our soft turbo detection schemes. Section IV is devoted to our energy efficiency

investigation. In Section V, we present our simulation results for investigating the achievable energy efficiency and the achievable BER. Our conclusions are offered in Section VI.

## II. SYSTEM MODEL

The paradigm shift to MIMO aided DSL communications allows us to conceive sophisticated MIMO signal processing techniques, such as precoding and/or postcoding applied for the transmitter and receiver, respectively. In this section, we consider the upstream transmission between the user and the Distribution Point Unit (DPU). Assuming that there is  $N$  upstream users and each of them are quipped with  $M$  pairs of twisted copper lines, which indicates that we have  $L = MN$ , where  $M = 1$  represents the simplest scenario of each group having a single pair of twisted lines. We assume that the Near-End Crosstalk (NEXT) has been completely canceled [27], hence the interference at the receiver is imposed by the Far-End Crosstalk (FEXT). Upon assuming that the Cyclic Prefix (CP) is sufficiently long for eliminating the inter-carrier interference, we can process the multi-tone signals on a per tone basis [28]. More particularly, the vector  $\mathbf{Y}_k \in \mathbb{C}^{L \times 1}$  of received signals on  $k$ -th tone consists of  $N$  vectors of  $\mathbf{Y}_{k,n} \in \mathbb{C}^{M \times 1}$ , which is given by

$$\mathbf{Y}_k = \sqrt{P_{t/k}} \mathbf{H}_k \mathbf{X}_k + \mathbf{W}_k, \quad (1)$$

where  $P_{t/k} = P_t/K$  is the power allocated to a single tone of a single channel,  $P_t$  is the total power transmitted over  $K$  subcarriers allocated to a single channel,  $\mathbf{H}_k \in \mathbb{C}^{L \times L}$  is the  $k$ -th tone DSL channel matrix subjected to FEXT,  $\mathbf{X}_k \in \mathbb{C}^{L \times 1}$  is the transmitted signal vector on tone  $k$  and  $\mathbf{W}_k \in \mathbb{C}^{L \times 1}$  is the noise vector. The elements  $W_{k,l}$ ,  $l = 1, 2, \dots, L$  of the additive noise contributions  $\mathbf{W}_k$  are i.i.d. and obey the distribution of  $\mathcal{CN}(0, \sigma_w^2)$ . More specifically,  $\mathbf{H}_k$  and  $\mathbf{X}_k$  can be expanded as

$$\mathbf{H}_k = \begin{bmatrix} \mathbf{H}_{k,1}^1 & \mathbf{H}_{k,1}^2 & \cdots & \mathbf{H}_{k,1}^N \\ \mathbf{H}_{k,2}^1 & \mathbf{H}_{k,2}^2 & \cdots & \mathbf{H}_{k,2}^N \\ \vdots & \vdots & \ddots & \vdots \\ \mathbf{H}_{k,N}^1 & \mathbf{H}_{k,N}^2 & \cdots & \mathbf{H}_{k,N}^N \end{bmatrix}, \quad (2)$$

$$\mathbf{X}_k = [\mathbf{X}_{k,1}^T, \mathbf{X}_{k,2}^T, \dots, \mathbf{X}_{k,N}^T]^T, \quad (3)$$

respectively. Furthermore,  $\mathbf{H}_{k,g}^n$  and  $\mathbf{X}_{k,n}$  are given by

$$\mathbf{H}_{k,g}^n = \begin{bmatrix} H_{k,g,1}^{n,1} & H_{k,g,1}^{n,2} & \cdots & H_{k,g,1}^{n,M} \\ H_{k,g,2}^{n,1} & H_{k,g,2}^{n,2} & \cdots & H_{k,g,2}^{n,M} \\ \vdots & \vdots & \ddots & \vdots \\ H_{k,g,M}^{n,1} & H_{k,g,M}^{n,2} & \cdots & H_{k,g,M}^{n,M} \end{bmatrix}, \quad (4)$$

$$\mathbf{X}_{k,n} = [X_{k,n,1}, X_{k,n,2}, \dots, X_{k,n,M}]^T, \quad (5)$$

where  $H_{k,n,m}^{n,m}$ ,  $n = 1, 2, \dots, N$ ,  $m = 1, 2, \dots, M$  is the direct channel coefficient of the  $m$ -th channel of group  $n$ , while  $H_{k,g,m'_g}^{n,m_n}$ ,  $g \neq n$  represents the crosstalk coupling on the  $m'$ -th channel of group  $g$  imposed by the  $m$ -th wire line channel of group  $n$ . Explicitly, the superscript  $m_n$  and the subscript  $m'_g$  are given by  $m_n = (n-1)M + m$ ,  $m'_g = (g-1)M + m'$ ,  $m, m' = 1, 2, \dots, M$ , whilst  $g$  and  $n$  indicate the

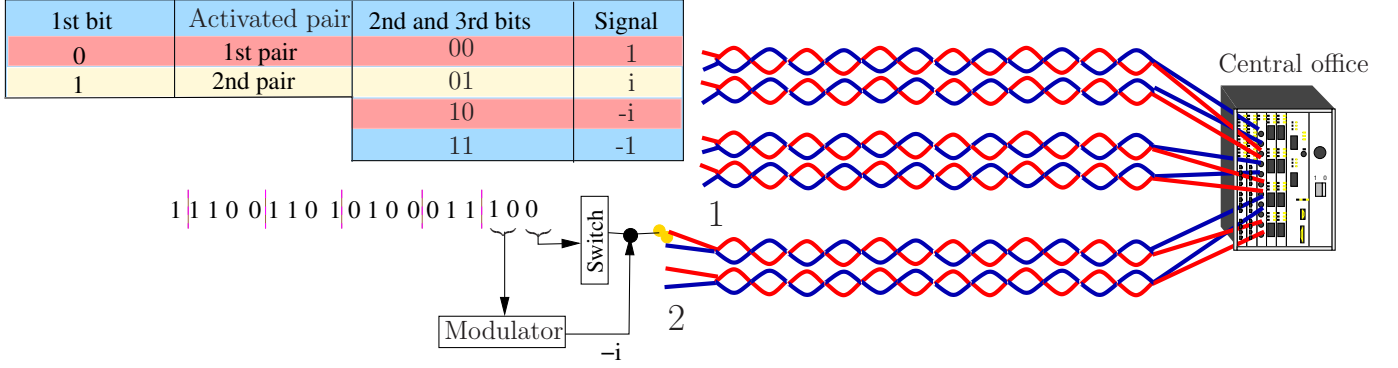


Fig. 1. An example of the proposed group-based SM for the upstream DSL system, which supports  $N = 3$  groups. Each group has  $M = 2$  twisted pairs and the classical delivered signals are selected from the QPSK constellation.

group indices. Moreover,  $H_{k,n,m'_n}^{n,m_n}$  is the intra-group-crosstalk imposed by the lines within a group, while  $H_{k,g,m'_g}^{n,m_n}, g \neq n$  is inter-group-crosstalk imposed by other groups [29].

The received signal can be detected based on the Zero-Forcing (ZF) criterion [19] as follows

$$\begin{aligned}\hat{\mathbf{X}}_k &= \frac{1}{\sqrt{P_{t/k}}} \mathbf{H}_k^{-1} \mathbf{Y}_k, \\ &= \mathbf{X}_k + \frac{1}{\sqrt{P_{t/k}}} \mathbf{H}_k^{-1} \mathbf{W}_k.\end{aligned}\quad (6)$$

We re-number the row and column indices of  $\mathbf{H}_k$  as  $\alpha$  and  $\beta$ , respectively, for simplifying the notation, where the mapping relationship between  $H_{k,\alpha}^\beta$  and  $H_{k,l,m}^{n,m'}$  is given by

$$g = \lfloor \frac{\alpha}{M} \rfloor + 1, \quad (7)$$

$$m = (\alpha - 1) \bmod M + 1, \quad (8)$$

$$n = \lfloor \frac{\beta}{M} \rfloor + 1, \quad (9)$$

$$m' = (\beta - 1) \bmod M + 1, \quad (10)$$

where  $\lfloor x \rfloor$  is a floor function, which returns the maximum integer less than  $x$ , and  $(x \bmod M)$  returns the remainder after division of  $x$  by  $M$ . Furthermore,  $g$  and  $n$  represent the group indices, while  $m$  and  $m'$  represent the channel indices within each group.

### III. PROPOSED GROUP-BASED SPATIAL MODULATION FOR DSL COMMUNICATIONS

Again, the grouped SM scheme proposed supports  $N$  upstream groups transmitted from the DPU to the central office. Each group has  $M$  twisted pairs, but only a single pair is activated for transmission in each group, while the remaining  $(M-1)$  pairs remain inactive, hence we can implicitly transmit  $p$  bits, where  $p = \log_2(M)$ . In this paper, we assume that  $M$  is a power of two. More specifically, the switch activates a pair using an “activation pattern”  $\mathbf{u}_{k,n,m_n}$ , which is a  $(M \times 1)$ -element binary unit vector, while the rest of the elements in  $\mathbf{u}_{k,n,m_n}$  are 0. We define the set of activation patterns as  $\mathbb{U}$ , which consists of  $M$  vectors. A logical ‘1’ in an activation pattern indicates that the corresponding channel is active and ‘0’ indicates that the corresponding channel is

silent. Then, the activated channel transmits  $q = \log_2(J)$  bits using the classic modulation alphabet  $\mathbb{A}$ , where  $J$  is the classic modulation order. For example, we have  $q = 2$  for Quadrature Phase Shift Keying (QPSK) and  $q = 3$  for 8-Quadrature-Amplitude Modulation (QAM). Therefore, the total number of bits conveyed by the proposed group-based SM is given by

$$\eta = N [\log_2(M) + \log_2(J)] = N[p + q], \quad (11)$$

where  $N$  is the number of simultaneously supported upstream groups, and each group is equipped with  $M$  twisted pairs.

The transmitted signal  $\mathbf{X}_{k,n} \in \mathbb{C}^{M \times 1}$  of group  $n$  in Eq. (5) becomes

$$\mathbf{X}_{k,n} = \mathbf{u}_{k,n,m_n} \cdot s_{k,n}, m_n = 1, 2, \dots, M, n = 1, 2, \dots, N, \quad (12)$$

where  $s_{k,n} \in \mathbb{A}$  is a modulated signal selected from the classic QAM constellation or Phase Shift Keying (PSK) constellation, while  $\mathbf{u}_{k,n,m_n}$  represents the  $m$ -th channel activated for transmission. Furthermore,  $\mathbf{X}_{k,n}$  is an element of  $\mathcal{S}_0$  and there are  $(JM)$  elements in  $\mathcal{S}_0$ .

Recalling Eq. (3) and Eq. (12), the transmitted signal vector  $\mathbf{X}_k \in \mathbb{C}^{MN \times 1}$  in Eq. (1) consists of  $\mathbf{X}_{k,n}, n = 1, 2, \dots, N$ , which can be rewritten as

$$\mathbf{X}_k = [\mathbf{X}_{k,1}, \mathbf{X}_{k,2}, \dots, \mathbf{X}_{k,N}]^T, m_n = 1, 2, \dots, M, \quad (13)$$

where  $\mathbf{X}_k$  is an element of  $\mathcal{S}$  and there are  $(JM)^N$  elements in  $\mathcal{S}$ .

*Example 1:* When  $N = 3$  and  $M = 2$ , the number of bits that can be conveyed by the line activation pattern is  $p = \log_2(M) = 1$  bits. The set of activation patterns is given by

$$\mathbb{U} = \left\{ \underbrace{\begin{bmatrix} 0 \\ 1 \end{bmatrix}}_0, \underbrace{\begin{bmatrix} 1 \\ 0 \end{bmatrix}}_1 \right\}, \quad (14)$$

where the position of ‘1’ in the vector represents the index of the activated channel.

The activated channels deliver QPSK signals conveying the following bits

$$\mathbb{A} = \left\{ \underbrace{1}_{00}, \underbrace{i}_{01}, \underbrace{-1}_{11}, \underbrace{-i}_{10} \right\}. \quad (15)$$

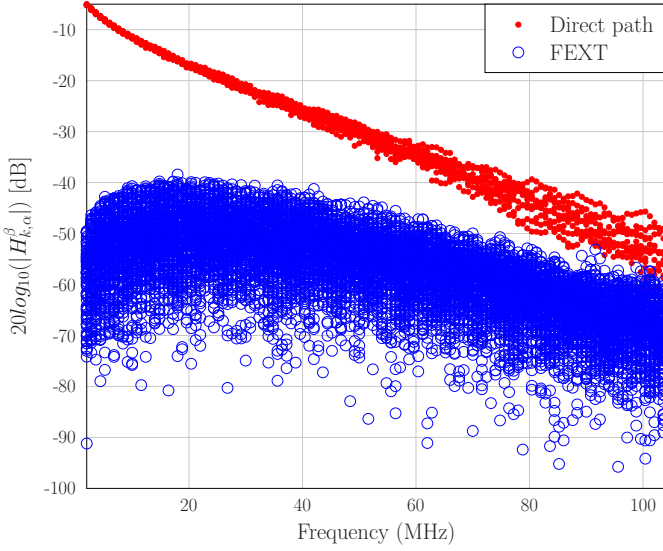


Fig. 2. Measurement of the crosstalk channel of a 200 meter BT cable consisting of 10 twisted copper pairs.

As illustrated in Fig. 1, the first bit is input into the switcher of Fig. 1, which activates the corresponding channel according to the activation pattern. The following two bits are input into the modulator, which outputs QPSK modulated signals.

#### A. Hard detection for group-based SM over DSL

At the receiver side, the optimal Maximum Likelihood (ML) principle can be employed for detecting the activated channels and the transmitted signals, which is formulated as

$$(\hat{\mathbf{m}}_k, \hat{\mathbf{s}}_k) = \arg \min_{\mathbf{m} \in \mathbb{M}^N, \mathbf{s} \in \mathbb{A}^N} \left\| \mathbf{Y}_k - \sqrt{P_{t/k}} \mathbf{H}_k \mathbf{X}_k \right\|_2^2, \quad (16)$$

where  $\mathbb{M} = \{1, 2, \dots, M\}$ ,  $\mathbf{m} = [m_1, m_2, \dots, m_N]^T$  has  $|\mathbb{M}|^N = M^N$  potential combinations for the activated channels, while  $\mathbf{s} = [s_1, s_2, \dots, s_N]^T$  has  $|\mathbb{A}|^N = J^N$  potential combinations of the transmitted signals delivered by  $N$  groups. In order to acquire the optimal ML detection results, we have to enumerate  $M^N \times J^N = (JM)^N$  different combinations of the activated channels and of the classic transmitted signals, which is impractical for a large number of groups, while employing high-order modulation.

Serendipitously, the DSL channel subjected to crosstalk has the following CWDD property [19] below 80 MHz, which has also demonstrated by our experimental observation.

*Property 1 (Column-wise diagonal dominance):* The diagonal elements of the DSL channel suffering from crosstalk have the largest magnitude on each column of  $\mathbf{H}_k$ , which may be mathematically formulated as

$$\left| H_{k,\alpha}^\beta \right| \leq \left| H_{k,\alpha}^\alpha \right|, \forall \alpha \neq \beta. \quad (17)$$

Exploiting the CWDD property of the DSL channel, the computational complexity of the detection problem in Eq. (16) can be significantly reduced by sequentially detecting the activated channels and the classic transmitted signals.

Actually, the CWDD property of DSL channel indicates that  $\left| H_{k,\alpha}^\beta \right|^2 \ll \left| H_{k,\alpha}^\alpha \right|^2, (n', m') \neq (n'', m'')$ . This feature has

also been verified by our the measured results in the Ultra-Fast Lab of BT Group plc., as shown in Fig. 2. Explicitly, we measured the frequency response of a 200 meter BT cable consisting of 10 twisted copper pairs, where each wire has a diameter of 0.5 mm. The measurement results demonstrate the CWDD property of DSL, and the results also show a gradually decreasing ratio between the desired signal and the FEXT upon increasing the frequency.

Upon assuming that the  $m^*$ -th line is activated by group  $n^*$ , we have  $\alpha = (n^* - 1)M + m^*$ . Thus,

$$\begin{aligned} |Y_{k,\alpha}|^2 &= \left| \sum_{\beta=1}^{MN} \sqrt{P_{t,cl}} H_{k,\alpha}^\beta X_{k,\beta} + W_{k,\alpha} \right|^2 \\ &\geq \left| \sqrt{P_{t,cl}} H_{k,\alpha}^\alpha X_{k,\alpha} \right|^2 \\ &\quad - \left| \sqrt{P_{t,cl}} \sum_{\beta=1, \beta \neq \alpha}^{MN} H_{k,\alpha}^\beta X_{k,\beta} + W_{k,\alpha} \right|^2, \quad (18) \\ &= \left| \sqrt{P_{t,cl}} H_{k,\alpha}^\alpha X_{k,\alpha} \right|^2 - \\ &\quad \left| \sum_{n=1, n \neq n^*}^N \sum_{m=1}^M \sqrt{P_{t,cl}} H_{k,\alpha}^{n,m} X_{k,n,m} + W_{k,\alpha} \right|^2 \\ &\geq P_{t,cl} \left| H_{k,\alpha}^\alpha \right|^2 - P_{t,cl} \sum_{n=1, n \neq n^*}^N \sum_{m=1}^M \left| H_{k,\alpha}^{n,m} \right|^2 - \sigma_w^2, \quad (19) \end{aligned}$$

For  $\alpha' = (n^* - 1)M + m, m \neq m^*, m = 1, 2, \dots, M$ ,  $Y_{k,\alpha'}$  is given by

$$\begin{aligned} |Y_{k,\alpha'}|^2 &= \left| \sum_{\beta=1}^{MN} \sqrt{P_{t,cl}} H_{k,\alpha'}^\beta X_{k,\beta} + W_{k,\alpha'} \right|^2 \\ &= \left| \sum_{n=1}^N \sum_{m=1}^M \sqrt{P_{t,cl}} H_{k,\alpha'}^{n,m} X_{k,n,m} + W_{k,\alpha'} \right|^2 \\ &\leq P_{t,cl} \sum_{n=1}^N \sum_{m=1}^M \left| H_{k,\alpha'}^{n,m} \right|^2 + \sigma_w^2, \quad (20) \end{aligned}$$

Considering all the other potential noise contributions, using an increased white noise Power Spectral Density (PSD) of  $-140$  dBm/Hz [3] is reasonable for DSL, which indicates that the power of white noise is significantly lower than  $P_{t/k} \left| H_{k,\alpha}^\alpha \right|^2$ . Omitting the term of  $\sigma_w^2$  in Eq. (20) and exploiting the CWDD property of the DSL channel, we have

$$\begin{aligned} |Y_{k,\alpha}|^2 - |Y_{k,\alpha'}|^2 &= P_{t/k} \left| H_{k,\alpha}^\alpha \right|^2 - P_{t/k} \sum_{n=1, n \neq n^*}^N \sum_{m=1}^M \left| H_{k,\alpha}^{n,m} \right|^2 \\ &\quad - P_{t/k} \sum_{n=1}^N \sum_{m=1}^M \left| H_{k,\alpha'}^{n,m} \right|^2 > 0. \quad (21) \end{aligned}$$

Thus,  $|Y_{k,\alpha}|^2 > |Y_{k,\alpha'}|^2$ .

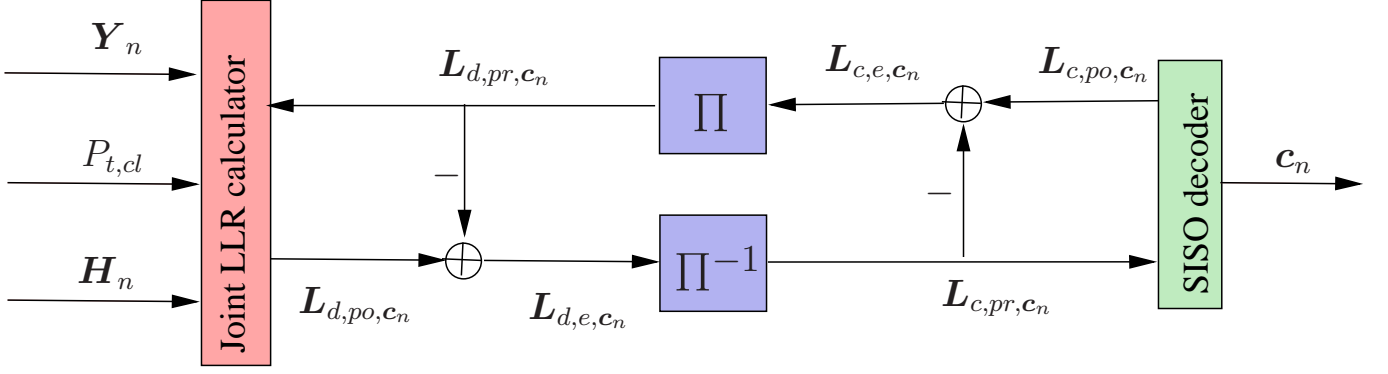


Fig. 3. Schematic of the SOSD-I. The subscripts  $d$  and  $c$  of  $L$  are associated with the LLR calculator and channel decoder, respectively, while the subscripts  $pr, po$  and  $e$  are used for representing the *a priori*, *a posteriori* and extrinsic information. The tone index of  $k$  is omitted in this figure for avoiding confusion.

Then, the activated channel of group  $u$  can also be detected on the basis of the group as follows

$$m_n = \arg \max_{m=\{1,2,\dots,M\}} |Y_{k,n,m}|^2, \quad (22)$$

where  $m_n$  indicates that the  $m_n$ -th channel is activated by group  $n$ . It was demonstrated in [30], [31] that Eq. (22) may result in error propagation in wireless channels. By contrast, due to the CWDD property of the DSL channel, the single-line-based SM detection of Eq. (22) effectively reduces the  $(MN)$ -variable problem-which is reminiscent of the wireless Vertical-Bell Laboratories Layered Space-Time (V-BLAST) detection problem- to an  $N$ -variable detection problem without suffering from error propagation. This is rather appealing feature of employing SM in DSL.

Note that  $|Y_{k,\alpha}|^2$ , may be less than  $|Y_{k,\alpha'}|^2$  when the DSL is very long or the frequency is very high, since the CWDD property of the DSL channel becomes less pronounced upon increasing the loop length or increasing the frequency, as seen in Fig. 2. This will result in a poor BER performance due to mis-detection of the activated channels, which will be investigated in Section V.

The activated channel indices are marked as a vector  $\mathbf{m}_k^* = [m_1, m_2, \dots, m_N]^T$ , where  $m_n = (n-1)M + m$ . Then the received signal model of Eq. (1) can be truncated as

$$\tilde{\mathbf{Y}}_k = \sqrt{P_{t/k}} \tilde{\mathbf{H}}_k \tilde{\mathbf{s}}_k + \tilde{\mathbf{W}}_k, \quad (23)$$

where  $\tilde{\mathbf{Y}}_k \in \mathcal{C}^{N \times 1}$ ,  $\tilde{\mathbf{s}}_k \in \mathcal{C}^{N \times 1}$  and  $\tilde{\mathbf{W}}_k \in \mathcal{C}^{N \times 1}$  only have the elements at the position  $\mathbf{m}_k^*$  of the vectors  $\mathbf{Y}_k$ ,  $\mathbf{X}_k$  and  $\mathbf{W}_k$ , respectively. Furthermore,  $\tilde{\mathbf{H}}_k \in \mathcal{C}^{N \times N}$  is a truncated version of  $\mathbf{H}_k$ , retaining its  $\mathbf{m}_k^*$  rows and  $\mathbf{m}_k^*$  columns.

Upon applying the ZF criterion, we arrive at the linear crosstalk canceler [19] formulated as:

$$\hat{\tilde{\mathbf{s}}}_k = \frac{1}{\sqrt{P_{t/k}}} \tilde{\mathbf{H}}_k^{-1} \tilde{\mathbf{Y}}_k, \quad (24)$$

$$= \tilde{\mathbf{s}}_k + \frac{1}{\sqrt{P_{t/k}}} \tilde{\mathbf{H}}_k^{-1} \tilde{\mathbf{W}}_k, \quad (25)$$

$$= \tilde{\mathbf{s}}_k + \tilde{\mathbf{W}}_k, \quad (26)$$

where  $\tilde{\mathbf{W}}_k = \frac{1}{\sqrt{P_{t/k}}} \tilde{\mathbf{H}}_k^{-1} \tilde{\mathbf{W}}_k$  and  $\tilde{\mathbf{W}}_{k,n}$  obeys the distribution

of  $\mathcal{CN}(0, \sigma_{\tilde{\mathbf{W}}_{k,n}}^2)$ , while  $\sigma_{\tilde{\mathbf{W}}_{k,n}}^2$  is given by

$$\sigma_{\tilde{\mathbf{W}}_{k,n}}^2 = \frac{1}{P_{t/k}} \left[ \tilde{\mathbf{H}}_k^{-1} \left( \tilde{\mathbf{H}}_k^{-1} \right)^H \right]_{n,n} \sigma_w^2. \quad (27)$$

In Eq. (27),  $[\cdot]_{n,n}$  represents the specific element on the  $n$ -th row and the  $n$ -th column.

### B. Soft turbo detection

In this subsection, we propose a pair of sub-optimal soft detection schemes for detecting both the active channels and the signals delivered by the active channels. The first scheme is termed as Sub-Optimal Soft Detection I (SOSD-I), which jointly detects the active channels and the classic symbols based on soft *a posteriori* information, as seen in Fig. 3. The second scheme is termed as Sub-Optimal Soft Detection II (SOSD-II), which separately detects the active channels by exploiting the CWDD property of the DSL channels and the classic symbols based on soft *a posteriori* information, respectively, as seen in Fig. 4. The soft information provided either by the SOSD-I or by the SOSD-II scheme is fed to a Soft-In Soft-Out (SISO) turbo decoder.

#### (1) Sub-Optimal Soft Detection I

The  $i$ -th bit carried by the channel of group  $n$  on tone  $k$  is denoted as  $a_{k,n}[i]$ , which represents the activation pattern vector mapped by the  $i$ -th bit of group  $n$  on tone  $k$ . For example,  $[00]$  is mapped to  $[0001]^T$ , indicating that the first channel is activated, while the  $i$ -th bit carried by the classic symbol of the active channel of group  $n$  on tone  $k$  is denoted as  $b_{k,n}[i]$ , which represents the  $M$ -QAM data stream mapped by the  $i$ -th bit of group  $n$  on tone  $k$ . For example  $[0000]$  is mapped to  $(-3 + 3j)$  in a system employing 16-QAM. We introduce the mapping of  $[a_{k,n}[1] \dots a_{k,n}[p] b_{k,n}[1] \dots b_{k,n}[q]]$  to  $[c_{k,n}[1] c_{k,n}[2] \dots c_{k,n}[(p+q)]]$ , where the first  $p$  bits of  $c_{k,n}$  are carried by the indices of the active channels, while the remaining  $q$  bits are carried by the signals delivered by the activated channels.

The Log-Likelihood Ratio (LLR) calculator delivers the *a posteriori* information of the bit  $c_{k,n}[i]$  expressed in terms of



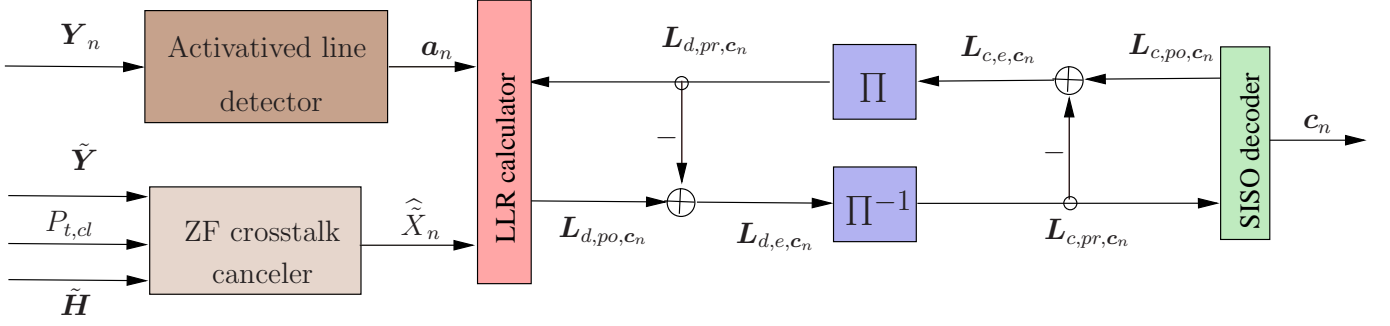


Fig. 4. Schematic of the SOSD-II. The subscripts  $d$  and  $c$  of  $L$  are associated with the LLR calculator and channel decoder, respectively, while the subscripts  $pr, po$  and  $e$  are used for representing the *a priori*, *a posteriori* and extrinsic information. The tone index of  $k$  is omitted in this figure for simplicity.

its LLR as [32], [33]

$$L_{po,c_{k,n}[i]} = \ln \frac{Pr[\mathbf{Y}_{k,n} | c_{k,n}[i] = 0]}{Pr[\mathbf{Y}_{k,n} | c_{k,n}[i] = 1]} + \ln \frac{Pr[c_{k,n}[i] = 0]}{Pr[c_{k,n}[i] = 1]},$$

$$= L_{e,c_{k,n}[i]} + L_{pr,c_{k,n}[i]}. \quad (28)$$

The second term of Equation (28) may be denoted by  $L_{pr,c_{k,n}[i]}$ , which represents the *a priori* LLRs of the interleaved and encoded bits  $c_{k,n}[i]$ . By contrast, the first term of Eq. (28), which is denoted by  $L_{e,c_{k,n}[i]}$  represents the extrinsic information delivered by the LLR calculator of Fig. 3. Explicitly, the extrinsic information  $L_{e,c_{k,n}[i]}$  is calculated based on the received signal  $\mathbf{Y}_{k,n}$  and on the *a priori* information concerning the encoded bits of group  $n$ , except for the  $i$ -th bit.

More specifically, the soft *a posteriori* information  $L_{po,c_{k,n}[i]}$  associated with bit  $b_{k,n}[i]$  can be approximated by the low-complexity Max-Log-MAP [34] as

$$L_{po,c_{k,n}[i]} = \max_{\substack{c_{k,n}[i]=0 \\ \forall \mathbf{X}_{k,n} \in \mathcal{S}_0}} d^i - \max_{\substack{c_{k,n}[i]=1 \\ \forall \mathbf{X}_{k,n} \in \mathcal{S}_0}} d^i, \quad (29)$$

where the probability metric  $d^i$  is given by

$$d^i = - \frac{\|\mathbf{Y}_{k,n} - \sqrt{P_{t/k}} \mathbf{H}_{k,n}^n \mathbf{X}_{k,n}\|_2^2}{2\sigma_w^2} + \sum_{j=1}^{(p+q)} \tilde{c}_{k,n}[j] L_{pr,c_{k,n}[j]}. \quad (30)$$

In Eq. (30),  $[\tilde{c}_{k,n}[1] \cdots \tilde{c}_{k,n}[p+q]] = \text{de2bi}(i)$  refers to the mapping of the SM bits to the signal  $\mathbf{X}_{k,n}$ , where  $\text{de2bi}(i)$  converts decimal integers to binary symbols.

## (2) Sub-Optimal Soft Detection II

By exploiting the CWDD property of the DSL channel, the activated channels may be separately detected according to the hard detection rule of Eq. (22). The bits carried by the indices of active channels are mapped to the *a posteriori* information as

$$\begin{cases} L_{po,a_{k,n}[i]} = -1 & \text{if } a_{k,n}[i] = 0, \\ L_{po,a_{k,n}[i]} = 1 & \text{if } a_{k,n}[i] = 1. \end{cases} \quad (31)$$

Furthermore, the LLR calculator delivers the *a posteriori* information of the bits  $b_{k,n}[i]$  as

$$L_{po,b_{k,n}[i]} = \max_{\substack{b_{k,n}[i]=0 \\ \forall \mathbf{X}_{k,n} \in \mathcal{S}_0}} d^i - \max_{\substack{b_{k,n}[i]=1 \\ \forall \mathbf{X}_{k,n} \in \mathcal{S}_0}} d^i, \quad (32)$$

where the probability metric  $d^i$  of SOSD-II is given by

$$d^i = - \frac{|\hat{s}_{k,n} - s_{k,n}|^2}{2\sigma_w^2} + \sum_{j=1}^q \tilde{b}_{k,n}[j] L_{pr,b_{k,n}[j]}. \quad (33)$$

In Eq. (33),  $[\tilde{b}_{k,n}[1] \cdots \tilde{b}_{k,n}[(p+q)]] = \text{de2bi}(i)$  represents the decimal to binary mapping of the signal  $s_{k,n}$  delivered.

## IV. CAPACITY AND ENERGY-EFFICIENCY ANALYSIS

In this section, we investigate both the CCMC and DCMC capacities, where the CCMC capacity is the maximum achievable rate of a given channel in case of Gaussian distributed transmitted signals. However, the DCMC capacity may be more practical for guiding the design of practical modulation schemes. Furthermore, the energy efficiency of the proposed group-based SM is investigated.

### A. CCMC Capacity analysis

The CCMC capacity of the MIMO channel is achieved by maximizing the mutual information between the input signal and output signal per channel, which is given by

$$C_{\text{CCMC}} = \max_{p(\mathbf{S})} \left[ \frac{1}{L} \mathcal{H}(\mathbf{Y}) - \frac{1}{L} \mathcal{H}(\mathbf{Y}|\mathbf{S}) \right]. \quad (34)$$

Thus, the CCMC capacity on tone  $k$  of a vectoring scheme [19] can be formulated as

$$C_k^{\text{vec}} = \mathbb{E} \left\{ \Delta_f \log_2 \det \left( \mathbf{I}_L + \frac{P_{t/k}^{\text{vec}}}{L\sigma_w^2} \mathbf{H}_k^H \mathbf{H}_k \right) \right\}, \quad (35)$$

where  $L = MN$  is the total number of channels of  $N$  users and  $\Delta_f$  is the bandwidth of a single tone.  $P_{t/k}^{\text{vec}}$  represents the power allocated to a single tone of a single channel for vectoring scheme.

Since SM conveys its information both via the classic constellation points of the modulated signal and by the spatial domain in the form of the activated line index, its capacity is given by the sum of the classic signal domain capacity and of the spatial domain capacity [35]. Thus, the capacity of the proposed group-based SM can be written as

$$C_{\text{SM},k,\text{total}} = \sum_{n=1}^N (C_{\text{signal},k,n} + C_{\text{spatial},k,n}), \quad (36)$$

$$C_{\text{spatial},n} = \frac{1}{M} \sum_{m=1}^M \mathbb{E} \left\{ \log_2 \frac{\frac{M}{1 + \frac{P_{t/k}^{\text{SM}} \|\mathbf{H}_k^{n_m}\|^2}{\sigma_w^2}} \exp \left( -\mathbf{Y}_{k,n} \left( P_{t/k}^{\text{SM}} \mathbf{H}_k^{n_m, \text{H}} \mathbf{H}_k^{n_m} + \sigma_w^2 \mathbf{I}_M \right)^{-1} \mathbf{Y}_{k,n}^{\text{H}} \right)}{\sum_{m'=1}^M \frac{1}{1 + \frac{P_{t/k}^{\text{SM}} \|\mathbf{H}_k^{n_{m'}}\|^2}{\sigma_w^2}} \exp \left( -\mathbf{Y}_{k,n} \left( P_{t/k}^{\text{SM}} \mathbf{H}_k^{n_{m'}, \text{H}} \mathbf{H}_k^{n_{m'}} + \sigma_w^2 \mathbf{I}_M \right)^{-1} \mathbf{Y}_{k,n}^{\text{H}} \right)} \right\}. \quad (40)$$

where  $C_{\text{signal},k,n}$  and  $C_{\text{spatial},k,n}$  represent the capacity of the signal domain and the capacity of the spatial domain, respectively.

More explicitly, the first term of Eq. (36) represents a single-input multiple-output (SIMO) system's capacity, which is maximized when the input is assumed to be a Gaussian-distributed continuous signal, formulated as:

$$\begin{aligned} C_{\text{signal},k,n} &= \max I(s_{k,n}; \mathbf{Y}_{k,n}|m), \\ &= \frac{\Delta_f}{M} \sum_{m=1}^M \log_2 \left( 1 + \frac{P_{t/k}^{\text{SM}} \|\mathbf{H}_k^{n_m}\|_2^2}{\sigma_w^2} \right), \end{aligned} \quad (37)$$

where  $I(s_{k,n}; \mathbf{Y}_{k,n}|m)$  is the mutual information between  $s_{k,n}$  and  $\mathbf{Y}_{k,n}$  conditioned on  $m$ ,  $P_{t/k}^{\text{SM}}$  represents the power allocated to a single tone of a single channel for group-based SM.

Similarly, the second term of Eq. (36) is also maximized by the Gaussian Probability Distribution Function (PDF) of the output signal as:

$$\begin{aligned} p(\mathbf{Y}_{k,n}|m) &= \frac{1}{\det(\pi \mathbf{R}_{\mathbf{Y}\mathbf{Y}|m})} \exp(-\mathbf{Y}_{k,n} \mathbf{R}_{\mathbf{Y}\mathbf{Y}|m}^{-1} \mathbf{Y}_{k,n}^{\text{H}}), \\ &= \frac{1}{\frac{\pi}{\sigma_w^2} \left( 1 + \frac{P_{t/k}^{\text{SM}} \|\mathbf{H}_k^{n_m}\|_2^2}{\sigma_w^2} \right)} \times \\ &\exp \left( -\mathbf{Y}_{k,n} \left( P_{t/k}^{\text{SM}} \mathbf{H}_k^{n_m, \text{H}} \mathbf{H}_k^{n_m} + \sigma_w^2 \mathbf{I}_M \right)^{-1} \mathbf{Y}_{k,n}^{\text{H}} \right). \end{aligned} \quad (38)$$

As a result, the second term of Eq. (36) may be further expressed as

$$\begin{aligned} C_{\text{spatial},k,n} &= \max I(m; \mathbf{Y}_{k,n}), \\ &= \max_{p(m)} \int \int p(\mathbf{Y}_{k,n}|m) p(m) \log_2 \left( \frac{p(\mathbf{Y}_{k,n}|m)}{P(\mathbf{Y}_{k,n})} \right) dm d\mathbf{Y}_{k,n}, \end{aligned} \quad (39)$$

where the average output PDF is given by  $p(\mathbf{Y}_{k,n}) = \int p(\mathbf{Y}_{k,n}|m) p(m) dm$ . Naturally, Eq. (39) is maximized when the input PDF  $p(m)$  is also Gaussian given that the power is constraint. However, the index  $m$  of the activated line is confined to the limited discrete range of  $(1 \leq m \leq M)$ , which cannot be generalized by allowing  $M$  to tend to infinity. As a remedy, according to [36], the activated lines index  $M$  may be interpreted as a discrete signal. Hence, Eq. (39) is maximized for equi-probable source of  $p(m) = \frac{1}{M}$  as

We note that Eq. (40) was also invoked for estimating the capacity of Space-Shift Keying (SSK) and Space-Time Shift Keying (STSK) in [37] and [38], respectively. Owing to the discrete nature of the activation index, it was demonstrated in [39] that SM suffers from a capacity loss compared to the Bell Laboratories Layer Space-Time (BLAST) scheme. Nonetheless, we will demonstrate in Section V-A that in DSL

systems SM is capable of outperforming the vectoring scheme<sup>1</sup> in terms of its energy efficiency quantified in terms of the CCMC capacity normalized by the power consumption in Mbps/J.

In summary, it can be seen in Eq. (36) that the CCMC capacity of SM is higher than that of its conventional SIMO counterpart, which was also observed in [40].

### B. DCMC capacity analysis

In practical digital telecommunication systems, the input signals are typically discrete QAM or PSK signals, instead of being continuous Gaussian-distributed. Moreover, the DCMC capacity is directly determined by the choice of modulation, which can be adaptively controlled. This feature can be exploited for providing different-rate services to different users.

The DCMC capacity of the MIMO channel is given by [36]

$$C = \max_{p(\mathbf{S}_i) \in \mathcal{S}} \sum_{i=1}^I \int p(\mathbf{Y}|\mathbf{S}_i) p(\mathbf{S}_i) \log_2 \frac{p(\mathbf{Y}|\mathbf{S}_i)}{\sum_{i=1}^I p(\mathbf{Y}|\mathbf{S}_i) p(\mathbf{S}_i)} d\mathbf{Y}, \quad (41)$$

where  $I$  is the number of signals in the set of  $\mathcal{S}$ , and  $p(\mathbf{Y}|\mathbf{S}_i)$  is given by

$$p(\mathbf{Y}|\mathbf{S}_i) = \frac{1}{(\pi \sigma_w^2)^{N_R}} \exp \left( -\frac{\|\mathbf{Y} - \sqrt{P_{t/k}} \mathbf{H} \mathbf{S}_i\|_2^2}{\sigma_w^2} \right). \quad (42)$$

Again, the maximum of Eq. (41) is achieved, when the input signal vectors  $\mathbf{S}_i$  are equiprobable, i.e.,  $p(\mathbf{S}_i) = \frac{1}{I}$  for  $\forall i = 1, 2, \dots, I$ . Then, the DCMC capacity of the MIMO channel quantified in Eq. (41) can be rewritten as

$$C = \frac{1}{I} \sum_{i=1}^I \mathbb{E} \left\{ \log_2 \frac{Ip(\mathbf{Y}|\mathbf{S}_i)}{\sum_{i'=1}^I p(\mathbf{Y}|\mathbf{S}_{i'})} \right\}. \quad (43)$$

Thus, the capacity on tone  $k$  of the proposed grouped SM can be written as

$$C_k^{\text{SM}} = \frac{\Delta_f}{(JM)^N} \sum_{i=1}^{(JM)^N} \mathbb{E} \left\{ \log_2 \frac{(JM)^N p(\mathbf{Y}_k^{\text{SM}} | \mathbf{S}_{k,i}^{\text{SM}})}{\sum_{i'=1}^{(JM)^N} p(\mathbf{Y}_k^{\text{SM}} | \mathbf{S}_{k,i'}^{\text{SM}})} \right\}, \quad (44)$$

<sup>1</sup>The vectoring scheme in DSL systems is equivalent to the BLAST scheme in wireless communication systems.

where  $K$  is the total number of tones, and again,  $\Delta_f$  is the bandwidth of a single tone, while  $p(\mathbf{Y}_k|\mathbf{S}_{k,i})$  is given by

$$p(\mathbf{Y}_k^{\text{SM}}|\mathbf{S}_{k,i}) = \frac{1}{(\pi\sigma_w^2)^{MN}} \exp\left(-\frac{\|\mathbf{Y}_k^{\text{SM}} - \sqrt{P_{t/k}^{\text{SM}}}\mathbf{H}_k\mathbf{S}_{k,i}\|^2}{\sigma_w^2}\right). \quad (45)$$

In Eq. (45),  $P_{t/k}^{\text{SM}}$  is the power allocated to a single tone of a single channel for the group-based SM scheme.

By contrast, the vectoring is a classic DCMC MIMO channel. Thus, its capacity on tone  $k$  is given by

$$C_k^{\text{vec}} = \frac{\Delta_f}{J^{N_R}} \sum_{i=1}^{J^{N_R}} \mathbb{E} \left\{ \log_2 \frac{J^{N_R} p(\mathbf{Y}_k^{\text{vec}}|\mathbf{S}_{k,i}^{\text{vec}})}{\sum_{i'=1}^{J^{N_R}} p(\mathbf{Y}_k^{\text{vec}}|\mathbf{S}_{k,i'}^{\text{vec}})} \right\}, \quad (46)$$

where  $N_R = MN$  represents the total number of received channels,  $\mathbf{S}_{k,i} \in \mathcal{S}_{\text{vec}}$  and  $\mathcal{S}_{\text{vec}}$  has  $J^{N_R}$  elements.

### C. Power consumption model and energy efficiency analysis for DSL

The total power consumption of a DSL transceiver is constituted by that of the digital front-end, of the analog front-end and of the LD [41]. The LD is responsible for outputting the transmit power  $P_t$  required for signal transmission, thus we only consider the power consumption of the LD, but neglect the power consumed by the digital front-end and the analog front-end in our ensuing energy efficiency analysis. There are various types LDs, but here we consider the popular class-AB LD power model, which can be characterized as [41]

$$P_{\text{LD}} = V_s \left( I_Q + \sqrt{\frac{2}{\pi} \frac{P_t}{R'_{\text{line}}}} \right) + P_{\text{Hybrid}}, \quad (47)$$

where  $V_s$  is the supply voltage of the LD,  $I_Q$  is the quiescent current,  $R'_{\text{line}}$  is the transformed resistance of the line, and  $P_{\text{Hybrid}}$  is the power consumed by the hybrid circuit.

For the sake of a fair comparison, all schemes are allocated the same power  $P_t^{\text{total}}$  for each group. Thus, the powers allocated to each of the active channels of the proposed group-based SM and to the vectoring are  $P_t^{\text{SM}} = P_t^{\text{total}}$ ,  $P_t^{\text{vec}} = \frac{P_t^{\text{total}}}{M}$ . Hence, the power consumption on each tone are  $P_{t/k}^{\text{SM}} = \frac{P_t^{\text{SM}}}{K}$  and  $P_{t/k}^{\text{vec}} = \frac{P_t^{\text{vec}}}{K}$  for the group-based SM and vectoring scheme, respectively.

Recalling that the proposed group-based SM only activates a single line in each group, while the vectoring activates all lines in each group, the energy efficiency of them on the  $k$ -th tone can be formulated as

$$\eta_k^{\text{vec}} = \frac{C_k^{\text{vec}}}{N P_{\text{LD},k}^{\text{vec}}}, \quad (48)$$

$$\eta_k^{\text{SM}} = \frac{C_k^{\text{SM}}}{N P_{\text{LD},k}^{\text{SM}}}. \quad (49)$$

where  $P_{\text{LD},k}^{\text{vec}} = P_{\text{LD}}^{\text{vec}}/k$  and  $P_{\text{LD},k}^{\text{SM}} = P_{\text{LD}}^{\text{SM}}/k$ . And  $P_{\text{LD}}^{\text{vec}}$  and  $P_{\text{LD}}^{\text{SM}}$  are calculated using Eq. 47 with the supplied transmit

TABLE I  
DEFAULT PARAMETERS USED FOR THE INVESTIGATED DSL COMMUNICATIONS.

Occupying frequency	2 MHz ~ 104.4 MHz
Number of tones $K$	2048
Bandwidth of a single tone $\Delta_f$	0.05 MHz
PSD of additive white Gaussian noise	-140 dBm/Hz
Number of groups $N$	2
Number of lines for each group $M$	2
Loop length	100 m (200 m)
Modulation order of vectored DSL $J_{\text{vec}}$	4
Supply voltage $V_s$	4 V
Quiescent current $I_Q$	11.1 mA
Transformed resistance of the line $R'_{\text{line}}$	64 $\Omega$
Power consumed by the hybrid circuit $P_{\text{Hybrid}}$	50 mW

power of  $P_t^{\text{vec}}$  and  $P_t^{\text{SM}}$ . Furthermore, the total energy efficient of all tones are given by

$$\eta^{\text{vec}} = \frac{\sum_{k=1}^K C_k^{\text{vec}}}{N P_{\text{LD}}^{\text{vec}}}, \quad (50)$$

$$\eta^{\text{SM}} = \frac{\sum_{k=1}^K C_k^{\text{SM}}}{N P_{\text{LD}}^{\text{SM}}}. \quad (51)$$

More especially, the energy efficient of the proposed group-based SM and the vectoring scheme are attained by replacing  $C_k^{\text{SM}}$  and  $C_k^{\text{vec}}$  with their corresponding CCMC capacity and DCMC capacity, respectively.

Note that both the SM's capacity is higher than that of a single DSL channel, but lower than that of the vectoring's capacity. However, SM only activates a single pair of twisted lines, which significantly reduces the power required for delivering information. These features facilitate for SM to have a better energy efficiency than that of vectoring.

## V. SIMULATION RESULTS

In this section, we investigate the achievable performance of the, CCMC capacity, DCMC capacity, energy efficiency and the BER. The vectoring scheme [19] is included as benchmark. The direct and crosstalk channels were characterized by the measurements of the UK BT Group plc. The measured channels consist of 2048 subchannels spanning from 2 MHz to 104.4 MHz, where each subchannel occupies 0.05 MHz. Again, the PSD of the additive white Gaussian noise (AWGN) is set to -140 dBm/Hz by considering all potential noise contributions [3]. The range of power investigated is  $3\text{dBm} \leq P_t \leq 30\text{dBm}$  allocated for each user over the 2048 subcarriers. Explicitly, the transmit power  $P_t$  will be equally shared by the  $M$  activated copper pairs of each user, saying  $P_t^{\text{SM}} = P_t$  for the proposed group-based SM transmission and  $P_t^{\text{vec}} = P_t/M$  for the vectoring scheme. The energy efficient is calculated by considering the total power consumption for generating a transmit power that consumed by the LD. Again, the LD's power consumption is obtained via Eq. (47). The values of the supply voltage, the quiescent current and the transformed resistance of the line are [41]  $V_s = 4$  V,



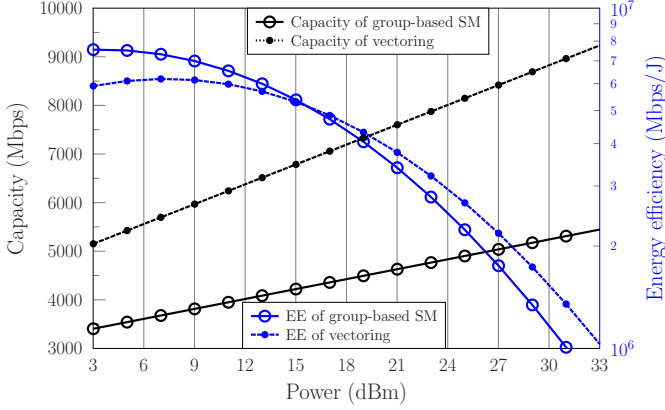


Fig. 5. Energy efficiency when operating exactly at the CCMC capacity at a DSL length of 100 m. The results were calculated by substituting Eq. (40) and Eq. (41) into Eq. (55) and Eq. (56), respectively.

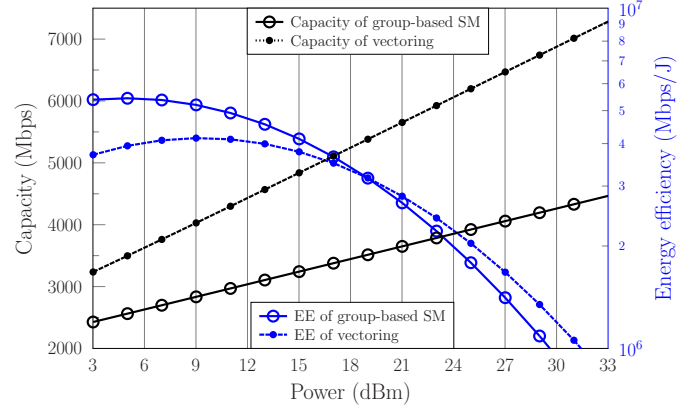


Fig. 6. Energy efficiency when operating exactly at the CCMC capacity at a DSL length of 200 m. The results were calculated by substituting Eq. (40) and Eq. (41) into Eq. (55) and Eq. (56), respectively.

$I_Q = 11.1$  mA and  $R'_{\text{line}} = 64 \Omega$ , respectively. Furthermore, the power consumed by the hybrid circuit is  $P_{\text{Hybrid}} = 50$  mW, as summarized in Table I. The number of twisted pairs used for each group is  $M = 2$ . Unless otherwise specified, these default parameter values of Table I were used throughout the simulations.

#### A. Energy efficiency analysis based on CCMC

In this subsection, we investigate the achievable CCMC capacity and energy efficiency. The energy efficiency is calculated based on the achievable CCMC capacity when operating exactly at loop lengths of 100 m and 200 m, as shown in Fig. 5 and Fig. 6, respectively. Explicitly, both the CCMC capacity and the energy efficient share the same x-axis, namely the transmit power<sup>2</sup>. The CCMC capacities are represented by the black lines and are quantified on the left-y-axis, while the energy efficient are exhibited by the blue lines measured on the right-y-axis.

It can be seen from Fig. 5 and Fig. 6 that the vectoring scheme outperforms the proposed group-based SM in term of CCMC capacity at the loop length of 100 m and 200m. However, the proposed group-based SM outperforms the vectoring scheme in term of energy efficient when the transmit powers are lower than 15 dBm at the loop length of 100 m and lower than 19 dBm at the loop length of 200m, respectively. Moreover, upon comparing Fig. 5 and Fig. 6, we can infer that the energy efficiency of all the two schemes considered becomes worse upon increasing the loop length. Furthermore the proposed group-based SM remains the better than the vectoring scheme in a wider range of transmit power.

#### B. Energy efficiency analysis based on DCMC

The achievable energy efficiency associated with operating at the DCMC capacity is investigated in this subsection. Firstly, we compare the total capacity of the proposed group-based SM and of the vectoring scheme. Furthermore, the impact of the loop length, of the number of simultaneous serviced

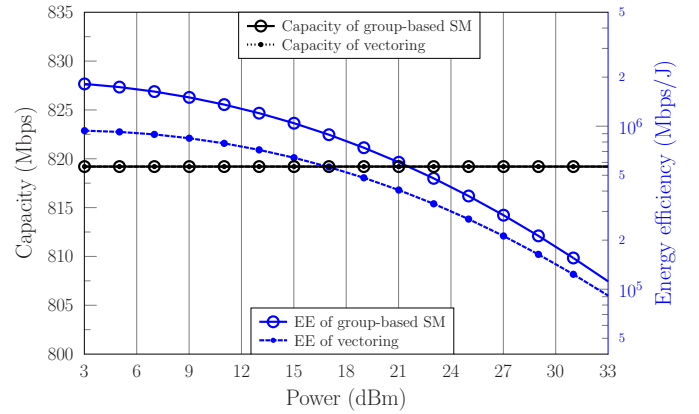


Fig. 7. Energy efficiency when operating exactly at the DCMC capacity at loop length of 100 m. The results were calculated by substituting Eq. (51) and Eq. (49) into Eq. (55) and Eq. (56), respectively.

and the number of the modulation order are investigated in Fig. 7 and Fig. 8, respectively. The default modulation of the vectoring scheme is 4-QAM for the investigation in Fig. 7 and Fig. 8. In order to achieve the same bit rate as the vectoring scheme, the default modulation mode of the group-based SM is 8-QAM. Unless otherwise specified, these default modulations are used throughout this subsection.

Fig. 7 portrays the energy efficiency when operating exactly at the DCMC capacity at the loop length of 100 m. We can see that the group-based SM outperforms the vectoring scheme at all of the examined transmit power range. More specifically, the proposed group-based outperforms the vectoring scheme at about  $5.7 \times 10^5$  Mbps/J in term of energy efficient. By contrast, the achievable DCMC capacities of the proposed group-based SM and the vectoring scheme are almost same, both of them have arrived at their saturated capacities of 819.2 Mbps at the loop length of 100m for the whole examined transmit power range. Furthermore, the energy efficient gap between the proposed group-based SM and the vectoring scheme becomes narrower and narrower upon increasing the transmit power.

Furthermore, by observing the energy efficiency in Fig. 8, we can see that the proposed group-based SM remains better than the vectoring scheme in term of energy efficient at the

<sup>2</sup>Again, the energy efficient is calculated by considering the total power consumed by the LD that generates the transmit power  $P_t$ .

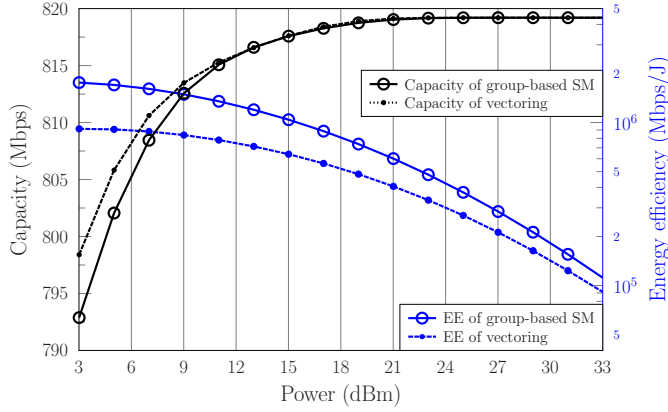


Fig. 8. Energy efficiency when operating exactly at the DCMC capacity at loop length of 200 m. The results were calculated by substituting Eq. (51) and Eq. (49) into Eq. (55) and Eq. (56), respectively.

loop length of 200 m. By contrast, the vectoring scheme outperforms the proposed SM in term of DCMC capacity in the transmit power range of [3dBm, 11dBm], and both of them achieve almost the same DCMC capacity when the transmit power is higher than 11 dBm.

### C. Energy efficiency on a specific tone

As observed in Fig. 2, both the direct path and the FEXT have different features at different frequencies (tones). In this subsection, we will investigate the achievable energy efficient on selected Representative tones. The PSD of the additive white Gaussian noise (AWGN) is set to  $-140$  dBm/Hz. The range of power allocated to each user is in the range of  $[0, 20]$  dBm, thus the power allocated to each tone is in the range of  $[-33.11, -13.11]$  dBm considering the equally power allocation for all the tones. Again, the energy efficient is calculated by considering the total power consumption for generating a transmit power that consumed by the LD, as seen in Eq. (48) and Eq. (48). The selected tone for our investigation are 500-th, 1000-th, 1500-th and 2000-th tones associated with central frequencies of  $f_c = 26.975$  MHz,  $f_c = 51.975$  MHz,  $f_c = 76.975$  MHz and  $f_c = 101.975$  MHz. Moreover, we also consider longer loop length of the serviced DSL lines, saying the loop length of 400m.

The energy efficiency achieved when operating exactly at the CCMC for a loop length of 400 m is shown in Fig. 9. Observe that the proposed group-based SM outperforms the vectoring scheme at all the four subchannels investigated.

Fig. 10 portrays the energy efficiency when operating exactly at the DCMC capacity at the loop length of 400 m. We can see that the group-based SM outperforms the vectoring scheme at the four frequencies of  $f_c = 26.975$  MHz,  $f_c = 51.975$  MHz,  $f_c = 76.975$  MHz and  $f_c = 101.975$  MHz. More specifically, the normalized energy efficiency of the proposed group-based SM at the frequency of  $f_c = 26.975$  MHz is similar to that at  $f_c = 51.975$  MHz. The same phenomenon is also observed for the vectoring scheme at frequencies of  $f_c = 26.975$  MHz and  $f_c = 51.975$  MHz. Explicitly, the energy efficiency of the proposed group-based SM is about 2.5 times higher than that of the vectoring scheme

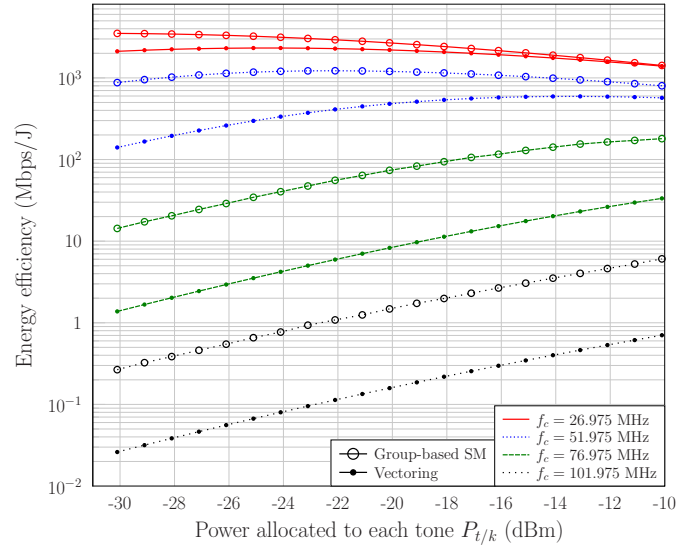


Fig. 9. Energy efficiency when operating exactly at the CCMC capacity at a DSL length of 400 m. The results were calculated by substituting Eq. (40) and Eq. (41) into Eq. (53) and Eq. (54), respectively.

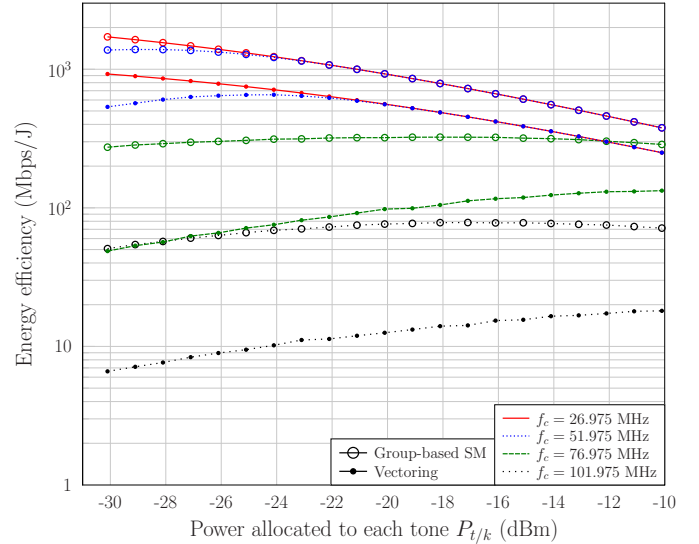


Fig. 10. Energy efficiency when operating exactly at the DCMC capacity at loop length of 400 m. The results were calculated by substituting Eq. (51) and Eq. (49) into Eq. (53) and Eq. (54), respectively.

at the frequency of  $f_c = 26.975$  and loop length of 400m. By contrast, the energy efficiency of the proposed group-based SM is about 1.4 times higher than that of the vectoring scheme at the lower transmission power assigned to the subchannel of  $f_c = 26.975$  at loop length 400m. The energy efficiency of the proposed group-based SM becomes about 2.5 times higher than that of the vectoring scheme at higher transmission powers.

Intuitively, the crosstalk becomes more serious upon increasing the number of twisted pairs. Hence the impact of crosstalk is investigated by increasing the number of twisted pairs in Fig. 11. Explicitly, in Fig. 11, we compare the achievable energy efficiency of  $N = 2$  and  $N = 3$  groups, where each group has  $M = 2$  twisted pairs. It can be seen from Fig. 11 that the proposed group-based SM aided trans-

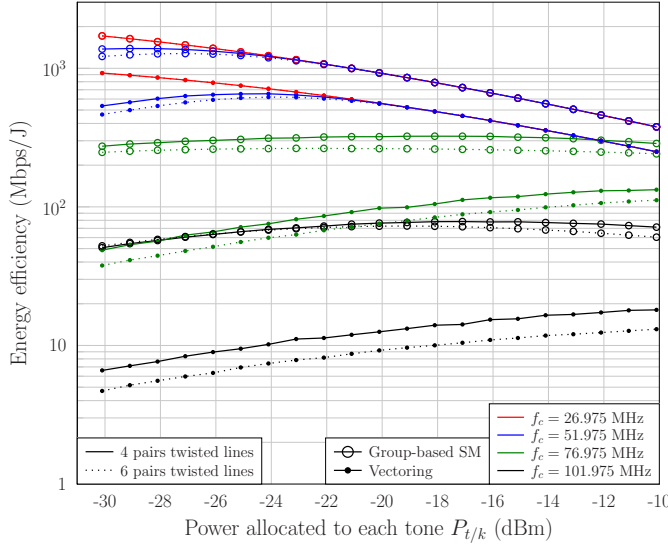


Fig. 11. Comparison of energy efficiency of ( $N = 2, M = 2$ ) and ( $N = 3, M = 2$ ) when operating at the DCMC capacity and at a loop length of 400 m. The results were calculated by substituting Eq. (51) and Eq. (49) into Eq. (53) and Eq. (54), respectively.

mission has almost the same energy efficiency at frequencies of  $f_c = 26.975$  MHz and  $f_c = 51.975$  MHz. However, the energy efficiency of the proposed group-based SM aided transmission becomes worse upon increasing the number of groups at frequencies  $f_c = 76.975$  MHz and  $f_c = 101.975$  MHz. The vectoring scheme exhibits a better energy efficiency at  $N = 2$  groups compared to  $N = 3$  groups at all the four frequencies of  $f_c = 26.975$  MHz,  $f_c = 51.975$  MHz,  $f_c = 76.975$  MHz and  $f_c = 101.975$  MHz. The energy efficiency comparison of Fig. 11 between  $N = 2$  groups and  $N = 3$  groups indicates that the vectoring scheme is more sensitive to the crosstalk.

Fig. 12 shows the energy efficiency at  $\eta = 6$  bits per group use (bpgu), which corresponds to modulation orders of  $J_{\text{vec}} = 8$  and  $J_{\text{sm}} = 32$  for vectoring scheme and group-based SM, respectively. The energy efficiency at a throughput of  $\eta = 4$  bpgu is included as benchmark for investigating the impact of the throughput. It can be seen from Fig. 12 that the proposed group-based SM shows the best energy efficiency at all the four representative investigated frequencies. The proposed group-based SM at  $\eta = 6$  bpgu shows a higher energy efficiency than at  $\eta = 4$  bpgu. However, the vectoring scheme at 6 bpgu has a higher energy efficiency than at  $\eta = 4$  at frequencies of  $f_c = 26.975$  MHz and  $f_c = 51.975$  MHz. By contrast, the vectoring scheme at  $\eta = 4$  bpgu has a higher energy efficiency than at  $\eta = 6$  bpgu at frequencies of  $f_c = 76.975$  MHz and  $f_c = 101.975$  MHz.

#### D. Comparison of BER performance

The achievable BER performance is investigated at the setting of transmit PSD =  $-70$  dBm/Hz for each group, which corresponds to the total transmit power of  $P_t^{\text{total}} = 10.10$  dBm over 2048 subchannels for each group, where each subchannel occupies 0.05 MHz. Note that the total transmit power is shared by  $M$  lines for a fair comparison.

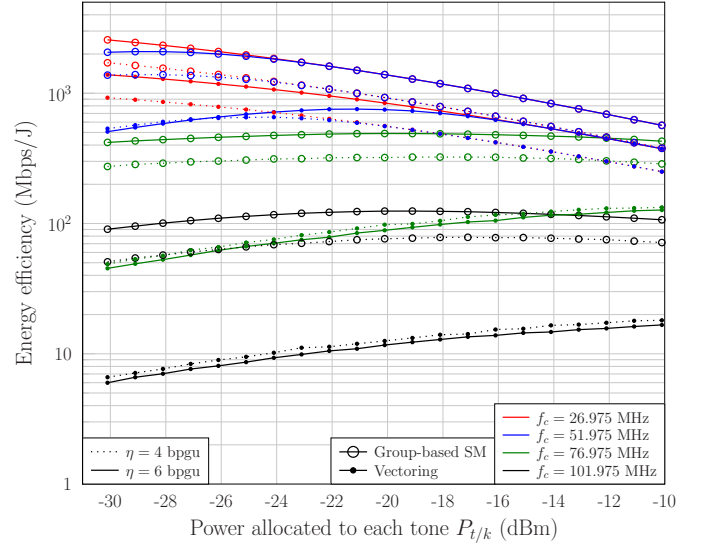


Fig. 12. Comparison of energy efficiency at  $\eta = 6$  bpgu based on the DCMC capacity at the loop length of 400m. The results were calculated by substituting Eq. (51) and Eq. (49) into Eq. (53) and Eq. (54), respectively.

Since the DSL channel qualities seen in Fig. 2 are quite different at low and high frequencies, we will investigate the achievable BER performance at a particular frequency first, and then we investigate the achievable BER performance upon increasing the bandwidth to the full bandwidth occupation of 102.4 MHz. The selected frequencies are  $f_c = 26.975$  MHz,  $f_c = 51.975$  MHz,  $f_c = 76.975$  MHz and  $f_c = 101.975$  MHz, which span from low frequency to high frequency.

It can be seen from Fig. 13 that the proposed SOSD-I outperforms vectoring scheme at the frequencies of  $f_c = 26.975$  MHz,  $f_c = 51.975$  MHz and  $f_c = 76.975$  MHz. Explicitly, at the BER level of  $1 \times 10^{-6}$ , the loop length gains achieved are about 37.5 m, 25 m and 9.4 m at  $f_c = 26.975$  MHz,  $f_c = 51.975$  MHz and  $f_c = 76.975$  MHz, respectively. This may be deemed to be almost identical, but bear in mind that this is achieved at a factor  $1/M = 1/2$  lower energy per group. Similarly, the reduced-complexity SOSD-II also outperforms the vectoring scheme at  $f_c = 26.975$  MHz and  $f_c = 51.975$  MHz. By contrast, at  $f_c = 76.975$  MHz and  $f_c = 101.975$  MHz, the proposed SOSD-II advocated only outperforms the vectoring scheme when the loops are longer than 248 m and 302 m, respectively, as reflected by the cross-over of their curves in Fig. 13. In order to clearly illustrate the gain achieved at a specific BER of  $10^{-6}$ , we summarize the DSL lengths of the three schemes considered in Table. II.

#### E. Overall performance

In this subsection, we investigate the overall achievable average BER (ABER) attained upon increasing the bandwidth, as shown in Fig. 14 and Fig. 15. It can be seen from Fig. 14 that both the proposed SOSD-I and the reduced complexity SOSD-II detection schemes exhibits a lower BER than the vectoring scheme right across the entire bandwidth examined at a DSL length of 400m. The same trend is also valid at the DSL length of 600 m.

TABLE II  
SUPPORTED TRANSMISSION LENGTH WHEN THE ACHIEVED BER IS AT  $10^{-6}$ .

Schemes \ Subchannels	$f_c = 26.975$ MHz	$f_c = 51.975$ MHz	$f_c = 76.975$ MHz	$f_c = 101.975$ MHz
SOSD-I	634.4 m	423.1 m	300 m	206.3 m
SOSD-II	600.0 m	407.2 m	281 m	212.5 m
Vectored DSL	605.0 m	400.0 m	293.0 m	234.4 m

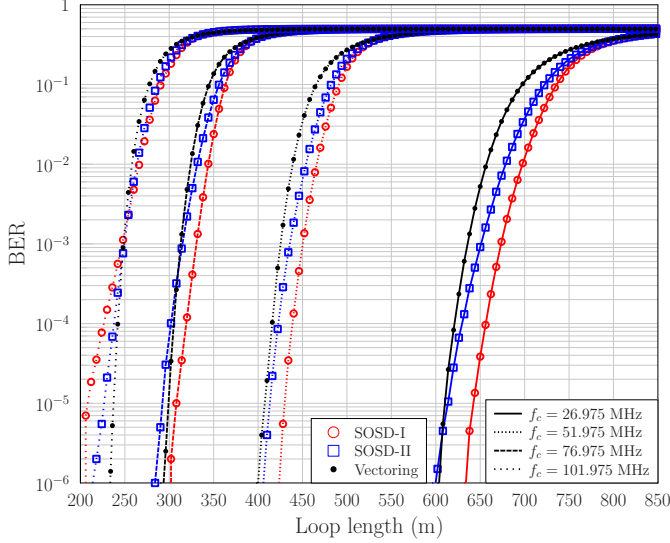


Fig. 13. BER performance versus loop length of group-based SM and vectored DSL. In the upstream multi-user DSL system considered, the number of group is  $N = 2$ , each group has  $M = 2$  twisted pairs. The bit rate is 4 bpgu per group, requiring that  $J_{\text{vec}} = 4$  and  $J_{\text{sm}} = 8$ .

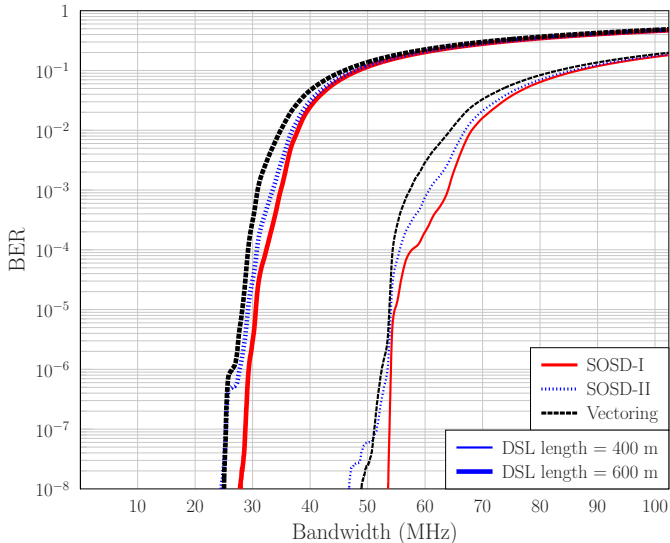


Fig. 14. Comparison of the total achievable capacity and the average BER upon increasing the bandwidth.

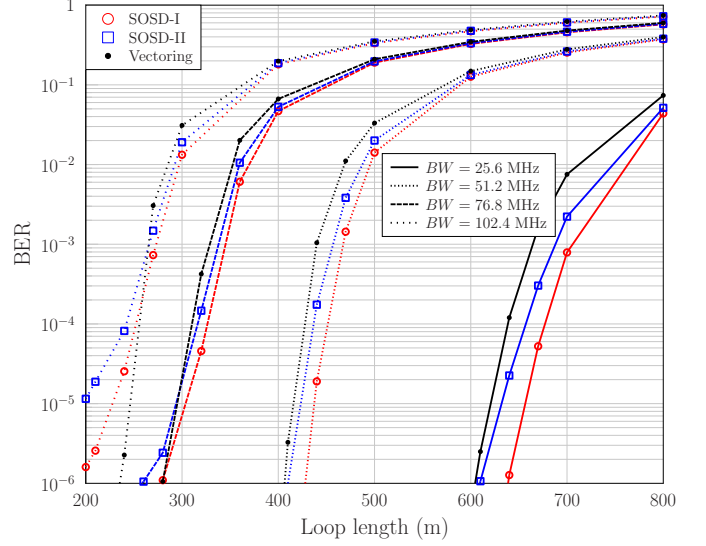


Fig. 15. Comparison of the average BER upon increasing the DSL length.

The overall BER performance upon increasing the cable length is quantified in Fig. 15. The proposed SOSD-I is capable of outperforming the vectoring scheme at the bandwidths of  $BW = 25.6$  MHz,  $BW = 51.2$  MHz and  $BW = 76.8$  MHz. However, at the bandwidth of  $BW = 102.4$  MHz, the SOSD-I only outperforms the vectoring scheme, when the DSL length becomes longer than 270 m. By contrast, the reduced complexity SOSD-II detection scheme is capable of outperforming the vectoring scheme at a bandwidth  $BW = 25.6$  MHz and bandwidth of  $BW = 51.2$  MHz. However, it only outperforms the vectoring scheme, when the DSL lengths are above 300 m and 270 m for the bandwidth of  $BW = 76.8$  MHz and  $BW = 102.4$  MHz, respectively. The observation of Fig. 15 shows that the SOSD-I and SOSD-II detection schemes have a better overall BER at longer DSL lengths. By contrast, the vectoring scheme only shows a better BER performance at shorter DSL lengths below 300 m and 270 m at bandwidths of  $BW = 25.6$  MHz and of  $BW = 51.2$  MHz, respectively.

## VI. CONCLUSIONS

In this paper, we proposed a group-based SM scheme for the multi-user upstream of DSL systems. Explicitly, we consider a emerging bonding scenario that customers have been equipped with two copper pairs. The twisted pairs are indexed and divided into groups, where each group only activates a single twisted pair in order to reduce the cross-talk and hence indirectly also the power consumption. This

is achieved by delivering “virtual bits” via identifying the index of the activated channel of each group. Furthermore, a pair of sub-optimal soft turbo detection schemes were proposed by exploiting the CWDD property of the DSL channel. The achievable energy efficiency was investigated, when operating exactly at the CCMC and DCMC capacities. Explicitly, the impact of loop length, the bit rate and of the binder channels was investigated by simulations. The proposed group-based SM exhibits the best energy efficiency for all the examined transmit powers and DSL loop lengths. Furthermore, the overall average BER were investigated upon increasing bandwidth, which showed that the group-based SM is capable of outperforming the vectoring scheme at lower frequencies and longer DSL loop lengths. Moreover, our investigations also showed that the vectoring scheme exhibited a better performance at very short DSL length, while both the proposed SOSD-I and the SOSD-II began to outperform the vectoring scheme for DSL lengths beyond 300 m and 270 m. This observation suggests the feasibility of a hybrid transmission scheme by exploiting the specific DSL channel characteristics in terms of its cable length and frequency as well as bandwidth used.

## REFERENCES

- [1] T. Bai, H. Zhang, J. Zhang, C. Xu, A. F. Al Rawi, and L. Hanzo, “Impulsive noise mitigation in digital subscriber lines: the state-of-the-art and research opportunities,” *IEEE Communications Magazine*, vol. 57, no. 5, pp. 145–151, May 2019.
- [2] V. Oksman, H. Schenk, A. Clausen, J. M. Cioffi, M. Mohseni, G. Ginis, C. Nuzman, J. Maes, M. Peeters, K. D. Fisher *et al.*, “The ITU-T’s new G.vector standard proliferates 100 Mb/s DSL,” *IEEE Communications Magazine*, vol. 48, no. 10, pp. 140–148, October 2010.
- [3] D. Acatauassu, I. Almeida, F. Muller, A. Klautau, C. Lu, K. Ericson, and B. Dortschy, *Measurement and Modeling Techniques for the Fourth Generation Broadband Over Copper, Advanced Topics in Measurements*. InTech, 2012.
- [4] J. Zhang, S. Chen, R. Zhang, A. F. A. Rawi, and L. Hanzo, “Differential evolution algorithm aided turbo channel estimation and multi-User detection for G. fast systems in the presence of FEXT,” *IEEE Access*, vol. 6, pp. 33 111–33 128, June 2018.
- [5] F. Mazzenga and R. Giuliano, “Analytical performance evaluation of VDSL2,” *IEEE Communications Letters*, vol. 21, no. 1, pp. 44–47, January 2017.
- [6] —, “Log-normal approximation for VDSL performance evaluation,” *IEEE Transactions on Communications*, vol. 64, no. 12, pp. 5266–5277, December 2016.
- [7] T. Bai, C. Xu, R. Zhang, A. F. Al Rawi, and L. Hanzo, “Performance of HARQ-Assisted OFDM Systems Contaminated by Impulsive Noise: Finite-Length LDPC Code Analysis,” *IEEE Access*, vol. 7, pp. 14 112–14 123, January 2019.
- [8] M. Guenach, C. Nuzman, J. Maes, M. Peeters, Y. Li, D. Van Bruyssel, and F. Defoort, “Power-efficient copper access,” *Bell Labs Technical Journal*, vol. 15, no. 2, pp. 117–129, 2010.
- [9] T. Bai, H. Zhang, R. Zhang, L.-L. Yang, A. F. Al Rawi, J. Zhang, and L. Hanzo, “Discrete multi-tone digital subscriber loop performance in the face of impulsive noise,” *IEEE Access*, vol. 5, pp. 10 478–10 495, June 2017.
- [10] V. Oksman, R. Strobel, X. Wang, D. Wei, R. Verbin, R. Goodson, and M. Sorbara, “The ITU-T’s new G.fast standard brings DSL into the Gigabit era,” *IEEE Communications Magazine*, vol. 54, no. 3, pp. 118–126, March 2016.
- [11] M. Wolkerstorfer, D. Statovci, and T. Nordström, “Dynamic spectrum management for energy-efficient transmission in DSL,” in *Proceedings of 11th IEEE Singapore International Conference on Communication Systems*. Guangzhou, China: IEEE, November 2008, pp. 1015–1020.
- [12] J. Baliga, R. Ayre, K. Hinton, and R. S. Tucker, “Energy consumption in wired and wireless access networks,” *IEEE Communications Magazine*, vol. 49, no. 6, pp. 70–77, June 2011.
- [13] O. Amin, E. Bedeer, M. H. Ahmed, and O. A. Dobre, “Energy efficiency–spectral efficiency tradeoff: A multiobjective optimization approach,” *IEEE Transactions on Vehicular Technology*, vol. 65, no. 4, pp. 1975–1981, April 2015.
- [14] K. B. Song, S. T. Chung, G. Ginis, and J. M. Cioffi, “Dynamic spectrum management for next-generation DSL systems,” *IEEE Communications Magazine*, vol. 40, no. 10, pp. 101–109, October 2002.
- [15] M. Guenach, C. Nuzman, J. Maes, and M. Peeters, “On power optimization in DSL systems,” in *Proceedings of IEEE International Conference on Communications Workshops*. Dresden, Germany: IEEE, June 2009, pp. 1–5.
- [16] —, “Trading off rate and power consumption in DSL systems,” in *Proceedings of IEEE GLOBECOM International Workshop on Green Communications*, Honolulu, US, November 2009, pp. 1–5.
- [17] M. Guenach, M. B. Ghorbel, C. Nuzman, K. Hooghe, M. Timmers, and J. Maes, “Energy management of DSL systems: Experimental findings,” in *Proceedings of IEEE Global Communications Conference*. Atlanta, USA: IEEE, December 2013, pp. 2779–2784.
- [18] G. Marrocco, M. Wolkerstorfer, T. Nordström, and D. Statovci, “Energy-efficient DSL using Vectoring,” in *Proceedings of IEEE Global Telecommunications Conference*. Houston, TX, USA: IEEE, December 2011, pp. 1–6.
- [19] R. Cendrillon, G. Ginis, E. Van den Bogaert, and M. Moonen, “A near-optimal linear crosstalk canceler for upstream VDSL,” *IEEE Transactions on Signal Processing*, vol. 54, no. 8, pp. 3136–3146, August 2006.
- [20] J. Maes and C. Nuzman, “Energy efficient discontinuous operation in vectored G. fast,” in *Proceedings of IEEE International Conference on Communications*. Sydney, Australia: IEEE, June 2014, pp. 3854–3858.
- [21] R. Y. Mesleh, H. Haas, S. Sinanović, C. W. Ahn, and S. Yun, “Spatial modulation,” *IEEE Transactions on Vehicular Technology*, vol. 57, no. 4, pp. 2228–2241, July 2008.
- [22] M. Di Renzo, H. Haas, A. Ghrayeb, S. Sugiura, and L. Hanzo, “Spatial modulation for generalized MIMO: Challenges, opportunities, and implementation,” *Proceedings of the IEEE*, vol. 102, no. 1, pp. 56–103, January 2014.
- [23] A. Stavridis, S. Sinanovic, M. D. Renzo, H. Haas, and P. Grant, “An energy saving base station employing spatial modulation,” in *Proceedings of IEEE 17th International Workshop on Computer Aided Modeling and Design of Communication Links and Networks*. Barcelona, Spain: IEEE, September 2012, pp. 231–235.
- [24] W. Coomans, R. B. Moraes, K. Hooghe, A. Duque, J. Galaro, M. Timmers, A. J. van Wijngaarden, M. Guenach, and J. Maes, “XG-fast: the 5th generation broadband,” *IEEE Communications Magazine*, vol. 53, no. 12, pp. 83–88, December 2015.
- [25] F. Vatalaro, F. Mazzenga, and R. Giuliano, “The sub-band vectoring technique for multi-operator environments,” *IEEE Access*, vol. 4, pp. 3310–3321, June 2016.
- [26] S. Galli, K. J. Kerpez, H. Mariotte, and F. Moulin, “PLC-to-DSL interference: Statistical model and impact on VDSL2, vectoring, and G. Fast,” *IEEE Journal on Selected Areas in Communications*, vol. 34, no. 7, pp. 1992–2005, July 2016.
- [27] R. Zidane, S. Huberman, C. Leung, and T. Le-Ngoc, “Vectored DSL: benefits and challenges for service providers,” *IEEE Communications Magazine*, vol. 51, no. 2, pp. 152–157, February 2013.
- [28] G. Ginis and J. M. Cioffi, “Vectored transmission for digital subscriber line systems,” *IEEE Journal on selected areas in communications*, vol. 20, no. 5, pp. 1085–1104, August 2002.
- [29] S. M. Zafaruddin, S. Prakriya, and S. Prasad, “Performance of linear minimum-output energy receiver for self and alien crosstalk mitigation in upstream vectored very high-speed digital subscriber line,” *IET Communications*, vol. 9, no. 6, pp. 862–871, April 2015.
- [30] C. Xu, S. Sugiura, S. X. Ng, and L. Hanzo, “Spatial modulation and space-time shift keying: optimal performance at a reduced detection complexity,” *IEEE Transactions on Communications*, vol. 61, no. 1, pp. 206–216, January 2013.
- [31] J. Jeganathan, A. Ghrayeb, and L. Szczecinski, “Spatial modulation: optimal detection and performance analysis,” *IEEE Communications Letters*, vol. 12, no. 8, pp. 545–547, August 2008.
- [32] J. Zhang, S. Chen, X. Mu, and L. Hanzo, “Turbo multi-user detection for OFDM/SDMA systems relying on differential evolution aided iterative channel estimation,” *IEEE Transactions on Communications*, vol. 60, no. 6, pp. 1621–1633, June 2012.
- [33] —, “Evolutionary-algorithm-assisted joint channel estimation and turbo multiuser detection/decoding for OFDM/SDMA,” *IEEE Transactions on Vehicular Technology*, vol. 63, no. 3, pp. 1204–1222, March 2014.



- [34] W. Koch and A. Baier, "Optimum and sub-optimum detection of coded data disturbed by time-varying intersymbol interference [applicable to digital mobile radio receivers]," in *Proceedings of IEEE Global Telecommunications Conference*. San Diego, US: IEEE, December 1990, pp. 1679–1684.
- [35] Y. Yang and B. Jiao, "Information-guided channel-hopping for high data rate wireless communication," *IEEE Communications Letters*, vol. 12, no. 4, April 2008.
- [36] S. Xin Ng and L. Hanzo, "On the MIMO channel capacity of multi-dimensional signal sets," *IEEE Transactions on Vehicular Technology*, vol. 55, no. 2, pp. 528–536, March 2006.
- [37] J. Jeganathan, A. Ghrayeb, L. Szczecinski, and A. Ceron, "Space shift keying modulation for MIMO channels," *IEEE Transactions on Wireless Communications*, vol. 8, no. 7, pp. 3692–3703, July 2009.
- [38] S. Sugiura, S. Chen, and L. Hanzo, "Coherent and differential space-time shift keying: A dispersion matrix approach," *IEEE Transactions on Communications*, vol. 58, no. 11, pp. 3219–3230, November 2010.
- [39] P. Yang, M. Di Renzo, Y. Xiao, S. Li, and L. Hanzo, "Design guidelines for spatial modulation," *IEEE Communications Surveys & Tutorials*, vol. 17, no. 1, pp. 6–26, Firstquarter 2015.
- [40] R. Rajashekar, K. Hari, and L. Hanzo, "Reduced-complexity ML detection and capacity-optimized training for spatial modulation systems," *IEEE Transactions on Communications*, vol. 62, no. 1, pp. 112–125, January 2014.
- [41] M. Wolkerstorfer, S. Trautmann, T. Nordström, and B. D. Putra, "Modeling and optimization of the line-driver power consumption in xDSL systems," *EURASIP Journal on Advances in Signal Processing*, vol. 2012, no. 1, pp. 1–15, January 2012.